CHAPTER II

THEORETICAL BACKGROUND AND LITERATURE SURVEY

2.1 Theoretical Background

2.1.1 Shear Deformation and Elongation Deformation

2.1.1.1 Shear deformation

In shear deformation a force (F) is applied tangentially to an elemental volume as shown in figure 2.1, so that the top layer is displaced by u. The relative displacement of the two layers is the simple shear strain (γ):

$$\gamma = \frac{u}{h} \tag{2.1}$$

The shear stress (force per unit area, τ) is given by:

$$\tau = \frac{F}{A} \tag{2.2}$$

For viscous flow it is more usual to consider the rate of strain, or shear rate, which given by:

$$\gamma = \frac{V}{H} \text{ or } \frac{dv}{dx} \tag{2.3}$$

Where, V is the velocity in the z direction.

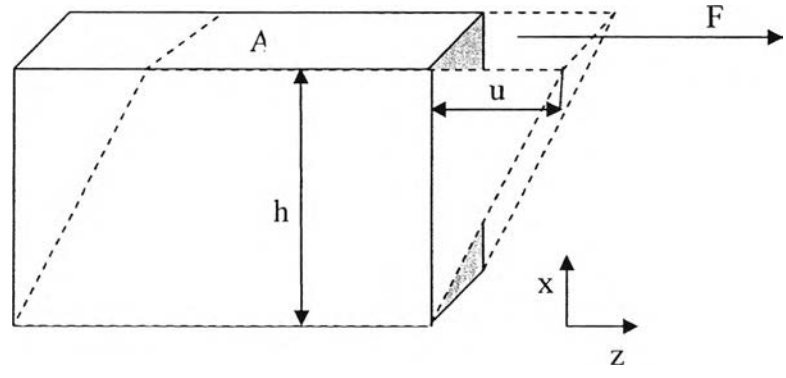

Figure 2.1 Geometry of the shear flow.

Polymer melts are viscoelastic in their response to an applied stress. Thus under certain conditions they will behave like a liquid, and will continuously deform while the stress is applied. Under other conditions the material behaves like an elastic solid, and on the removal of the applied stress there will be some recovery of the deformation. This viscoelastic response is illustrated in figure 2.2. It is necessary to define viscosity, which is a fundamental rheological parameter of fluids:

$$viscosity = (\eta) = \frac{\tau}{\dot{\gamma}} \tag{2.4}$$

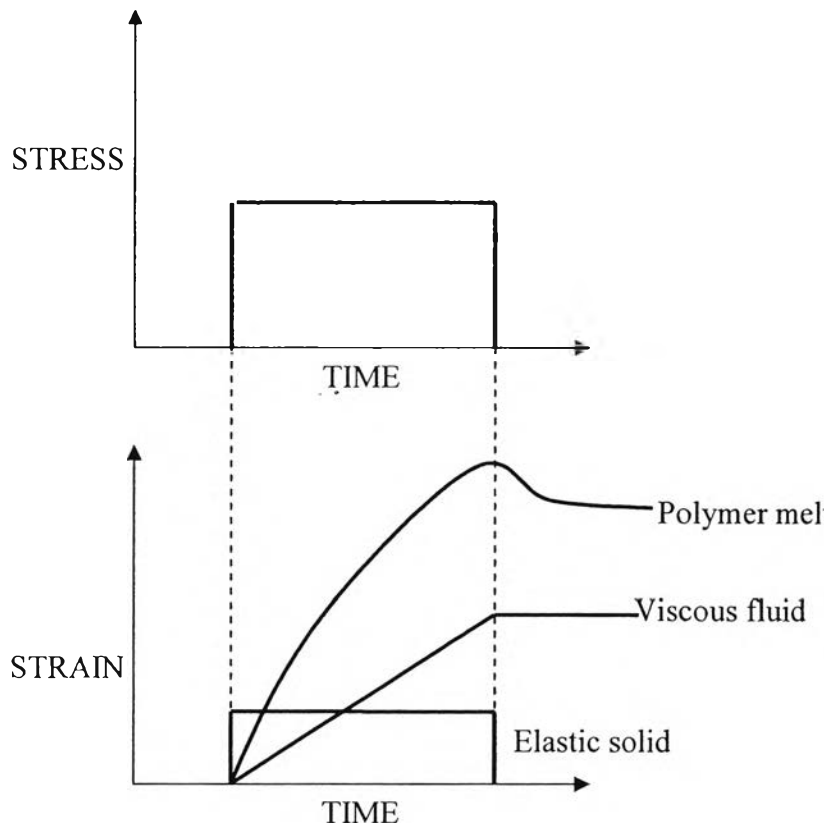

Figure 2.2 Viscoelastic behavior of the polymer melts.

2.1.1.2 Elongation deformation

This is achieved by applying a force normal to the opposite faces of the element, as indicated in figure 2.3 the tensile stress (σ) and the conventional engineering strain (ε) are given by:

$$\sigma = \frac{F}{A} \tag{2.5}$$

$$\varepsilon = \frac{l - l_0}{l_0} \tag{2.6}$$

Where l_0 the original length of the sample, and l is is the length at time t. Similarly, we can define an elongational strain rate ($\dot{\varepsilon}$), which is given by:

$$\dot{\varepsilon} = \frac{dv}{dz} \tag{2.7}$$

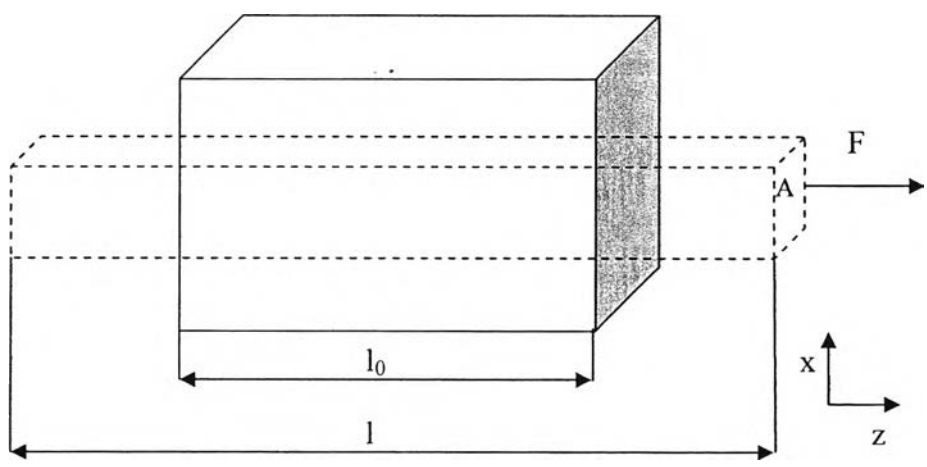

Figure 2.3 Geometry of elongational flow.

There is an increasing awareness of the significant of elongation flow but it has not been studied in the same detail as shear flow. This is mainly due to some associated experimental difficulties, and a general lack of awareness of its importance in practice. The elongational viscosity (η_e) of fluids is much higher than the shear viscosity and for the simple Newtonian fluids $\eta_e = 3.\eta_0$. The dependence of η_e on elongational rate is a function of polymer.

2.1.2 Capillary Rheometer

A very popular type of instrument for studying the rheological behavior of polymer melts is the capillary rheometer. As shown in Figure 2.4, a molten polymer is forced by a piston or by pressure from a reservoir, a barrel, through the capillary die. The quantity of polymer coming from the capillary per unit time at a given pressure drop is the basic measurement used to calculate the viscosity.

The capillary rheometer has a number of advantages. First, the instrument is easily filled up. This is an important consideration since most polymer melts are too viscous to pour readily even at high temperatures. The test temperature and rate of shear can vary in a wide range. The shear rate and flow geometry are similar to the conditions normally encountered in actual extrusion and injection molding. In addition to the viscosity, some indications of polymer elasticity can be obtained from the extrudate swell phenomenon. Finally, factors affecting the surface texture of the extrudate and the phenomenon of melt fracture can be studied. The main disadvantage of the capillary rheometer is that the rate of shear is not constant, but varies across the capillary. Another disadvantage is a number of corrections can be done concurrently, so the obtained rheological behavior is definitive.

Two corrections are commonly applied to capillary data in order to obtain the correct viscosity of polymeric fluids. The Rabinowitsch equation corrects the rate of shear at the wall for non-newtonian fluids. The power law factor (n) designates the dependence of shear stress over shear rate to n^{th} power. The Bagley correction takes care of non-ideality arising from viscous and elastic effects at the entrance of the capillary die. The effective length of the capillary is greater than its true length. The

Bagley correction factor should be independent of capillary length, but, in general, it does vary somewhat with L/R because of the elasticity of the polymer melts. The important equations pertaining to the capillary rheometer are:

$$\tau_{app} = \frac{rp}{2l} \tag{2.8}$$

Where τ_{app} is the apparent shear stress at the wall, r is the radius of the die, p is the pressure drop, l is the die length

$$\dot{\gamma} = \frac{4Q}{\pi r^3} \tag{2.9}$$

Where $\dot{\gamma}$ is the apparent shear rate, Q is volumetric flow rate of the compound materials, r is the radius of the die. Due to the accuracy of the data, and the limit of measurement, the correction of data was occurred as Bagley's correction (Bryson, 1970, Cogswell, 1994) and Rabinowitsch correction (Bryson, 1970, Cogswell, 1994).

$$\tau_{real} = \frac{rp}{2(l + nr)} = \frac{p}{2(l/r + n)} \tag{2.10}$$

Where τ_{real} is real shear stress, n is a multiplication factor from Bagley correction

$$\dot{\gamma}_{real} = \frac{3n+1}{4n}.\dot{\gamma} \tag{2.11}$$

Where $\dot{\gamma}_{real}$ is real shear rate, n is the slope on logarithm scale of apparent shear rate and apparent shear stress fitted in to Rabinowitsch correction. The viscosity of compound is given by the relation,

$$\eta = \frac{\tau_{real}}{\dot{\gamma}_{real}} \tag{2.12}$$

Where η is shear viscosity. The elongation value calculated according to the Cogswell's theory as followed,

$$N = \frac{\dot{\gamma}}{(4.\dot{\gamma}_{real} - 3.\dot{\gamma})} \tag{2.13}$$

$$P_e = (\tau_{app} - \tau_{real}).4.l / d \tag{2.14}$$

where N is an empirical constant, P_e is entry pressure, l is die length, d is die diameter, combined of eq. 2.13 and 2.14 to the relation of elongational rate, we get,

$$\varepsilon = \frac{4.\tau_{app}.\dot{\gamma}^2}{3(N+1)P_e} \tag{2.15}$$

Where ε is elongational rate, so that tensile stress can express,

$$\sigma = \frac{3(N+1)P_e}{8} \tag{2.16}$$

The elongational viscosity occurred on the eq.2.15 and 2.16 as,

$$\eta_{elong} = \frac{\sigma}{\varepsilon} \tag{2.17}$$

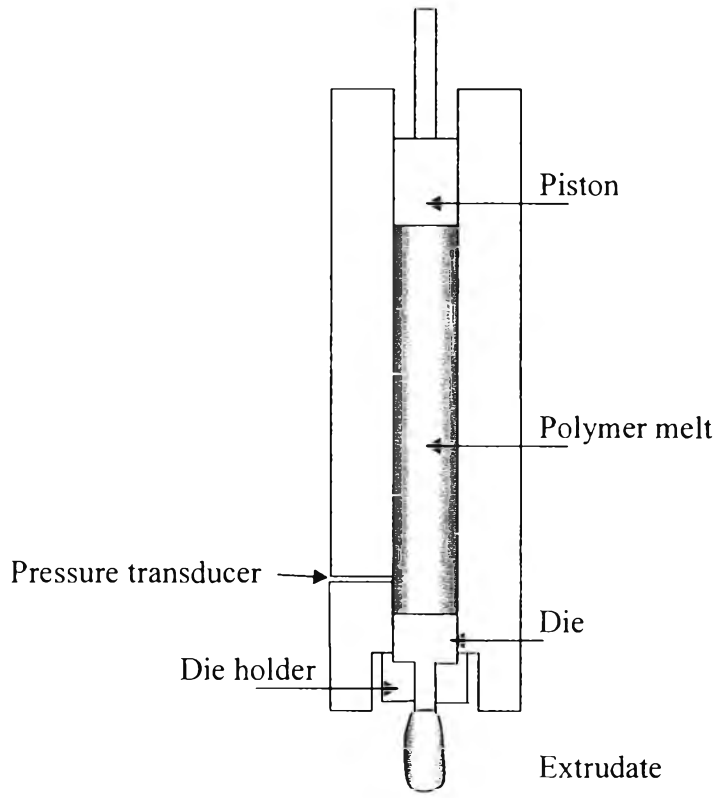

Figure 2.4 Schematic diagram of capillary rheometer.

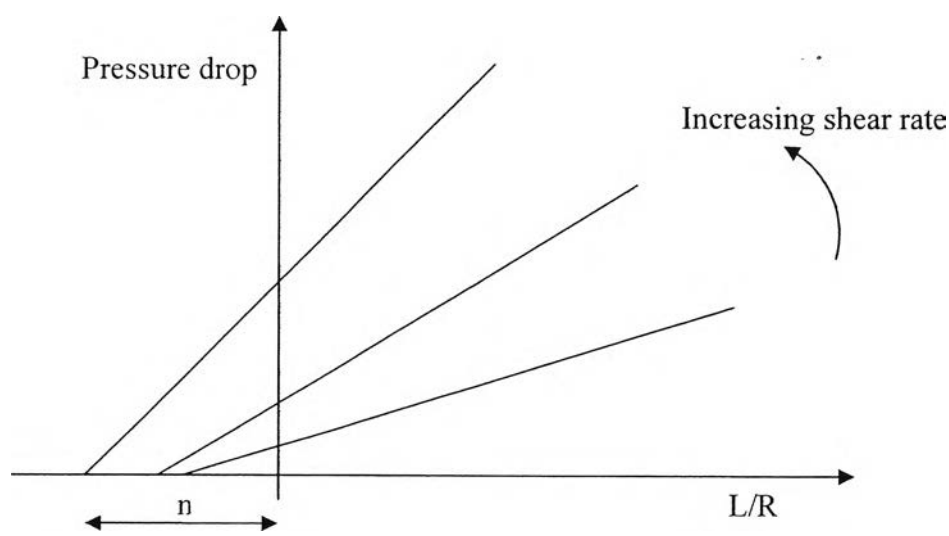

Figure 2.5 The Bagley correction for capillary rheometer.

2.1.3 Elastic Behavior of Polymer Melts.

The properties of the polymer are combination of the properties of an elastic solid and viscous fluid. During flow, they have ability to store energy and, when the stresses are removed, this strain is recoverable. For examples, when a simple liquid molecules slide past each other, the intermolecular attraction causes the formation of a drag force, the magnitude of which is reflected in the viscosity of the liquid. For high molecular weight polymers, the chains tend to uncoil as they are sheared. In addition, entanglements between molecules, to some extent, prevents the molecules slipping past each other in the normal way. When the molecules rest again, they tend to recoil, causing conformational relaxation to occur so the molecules take their original shape. These elastic processes are superimposed on the viscous flow and manifest themselves in a number of ways during polymer processing.

The most important effects which will be discussed here, are extrudate swell, sharkskin, and melt fracture.

2.1.3.1 Extrudate Swell

In capillary flow, the diameter of the extrudate is normally greater than the capillary diameter, a phenomenon known as extrudate or die swell. Normally, the extrudate swell is presented as the ratio of extrudate to die diameter (see Figure 2.6). Generally, extrudate swell relates to the elasticity of the polymer melts, but Newtonian fluids also exhibit a small amount of extrudate swell under certain conditions. Extrusion swell is important in extrusion and must be taken in to account by the die designer. The extent of extrudate swell depends on the applied stress and capillary length. At low values of L/R, the swell is dominated by elastic recovery from elongational stresses set up in the entry region. These stresses relax during flow down the capillary and thus extrudate swell decreases with increasing die aspect ratio. As L/R tends to infinity, extrudate swell reaches a constant value, where recovery from shear deformation becomes the dominating influence.

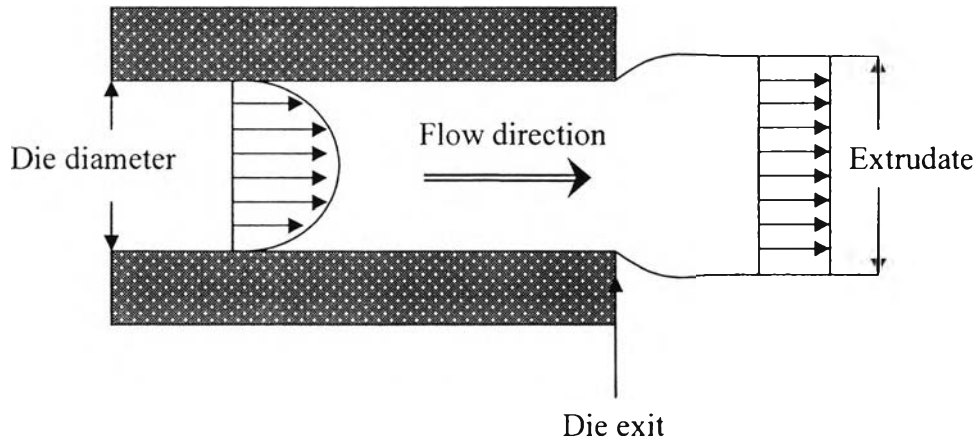

Figure 2.6 Schematic of extrudate swell.

Attempts to correlate extrudate swell with normal stress have been made by Metzner et al., whilst the correlations between the extrudate swell and end effect have been proposed with some success by Arai and Aoyama. A number of theories have been proposed to explain the extrudate swell but perhaps the most useful hypothesis is to assume that the molecules are oriented in the die and, on emergence into the atmosphere, recoiling takes place with the contraction in the direction of flow being offset by lateral expansion. If the leading ends of samples cut at the die face are examined, it is seen that they have a convex profile. Tanner has applied Lodge's entanglement theory (Lodge, 1964) to capillary flow and has obtained the following relationship between shear recovery and extrudate swell:

$$\left(\frac{R_j}{R}\right) = 0.1 + (1 + \gamma_R^2)^{1/6} \qquad (2.18)$$

Where γ_R the recoverable strain at is shear stress τ_R, and R_j is the radius of the extrudate

Using a different approach, Crowford [28] has developed the following expression:

$$\left(\frac{R_j}{R}\right)^2 = 0.67(\gamma_R)\left[\left(1 + \gamma_R^{-2}\right)^{3/2} - \gamma_R^{-3}\right] \qquad (2.19)$$

Prediction from the two theories, are very similar but neither accounts for the observed the extrudate swell in Newtonian fluids. For short die, Crowford has calculated the swell from the elastic recovery obtain from elongtional flow:

$$\left(\frac{R_J}{R}\right)^2 = \exp(\varepsilon_R) \tag{2.20}$$

Where ε_R is the recoverable strain from elongational flow under the tensile stress σ.

The extrudate swell tends to increase as $\bar{M}_w/\bar{M}_n$ increases and as long chains increases. This increase in the extrudate swell with the increase in long chain branching probably holds only for very long chains with molecular weight well beyond the critical molecular weight for entanglement. The filler tends to decrease the extrudate swell of polymers. The effect is most pronounced with rigid fillers, but even rubber and microgel particles, as in high impact ABS materials, can also decrease the extrudate swell. The explanation for this effect is not entirely clear since fillers do increase the shear modulus, but possibly change the flow process and decrease the relative importance of extensional flow at the entrance region to the capillaries. Another possibility is that the fillers increase the modulus so much that orientation of molecular segments is lessen. In any case, less elastic strain energy is stored in a polymer when filler particles are present. If the filler particles agglomerate which can be broken up and distributed well through a proper mixing, the extrudate swell increases with the extent of mixing.

The extrudate swell theories are not always accurate (especially when studying a flow through a complex die system during processing), but are in quantitative agreement with experimental data. In addition, the accurate measurement of swelling ratio has attracted the attention of a number of workers. They have been particularly concerned to avoid the effect of draw-down, contraction on cooling, and other influencing variables like crystallization.

2.1.3.2 Sharkskin

The surface irregularity known as sharkskin is characterized by a series of ridges perpendicular to the flow direction (see Figure 2.7). As a melt flows along the capillary die, a force required for the acceleration of the outer layer of the melt increases in order to equalize the melt velocity at the die exit. If the force exceeds the tensile strength of the melt, the melt will rupture and generate sharkskin as shown in Figure 2.8. The shark skin can occur at a lower extrusion rate than the melt fracture and depends very much on the temperature.

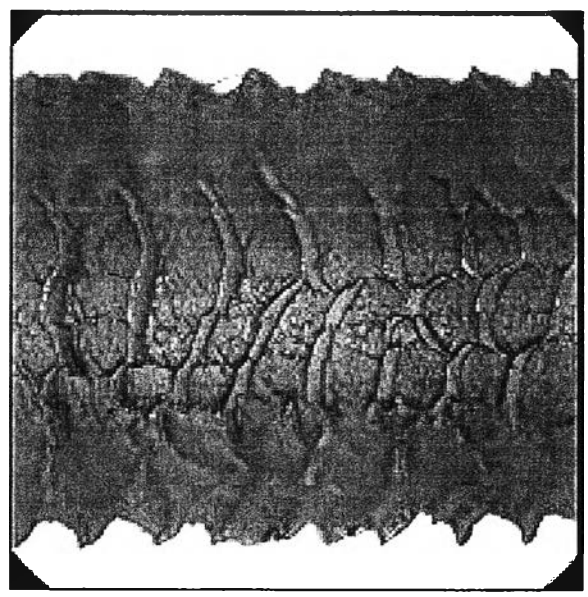

Figure 2.7 Sharkskin textures of the polymer melt.

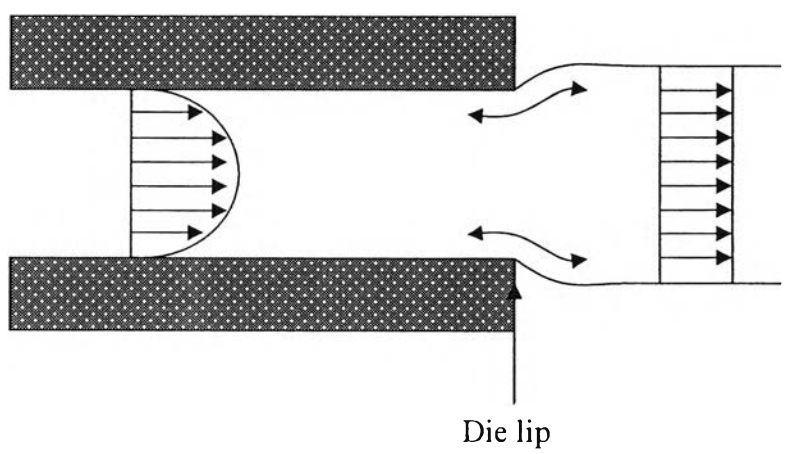

Figure 2.8 A mechanism showing the origins of sharkskin.

2.1.3.3 Melt Fracture

In capillary flow, the extrudate becomes irregular and distorted at high flow rates. This phenomenon so-called the melt fracture is complex and is associated with elastic behavior of the polymer melts. These vary important phenomenon which can affect the quality of the polymer products and their rate of production. Some examples of extrudate distortion that can occur are sketched in Figure 2.9. Melt fracture has been investigated under various test conditions and concluded to be affected by shear stress and shear rate, temperature, die materials and structure, and polymer molecular structure and its molecular weight. The mechanism of melt fracture is still not clear. A number of hypotheses have been proposed. Indeed, some leading workers in the field have at different times proposed different hypotheses. The first explanation was that this was a conventional turbulence effect that is similar to the simple liquids. Such turbulence occurred at Reynolds number of greater than about 2100, which is hardly achieved in the flow of polymer melts. It appears, therefore, that the conventional turbulence theory does not immediately fit the facts. The next is elastic effect theory, involving the fracture or tearing of molecular structure of the polymer melts at the die entrance. However, it has been shown that, with the turbulence of the melts, secondary flows (vortex) at the die entrance, the melt fracture does not always occur. Melt strength is the one of theory which relating that the shear rate or shear stress of the extrudate as it comes out of the die exceeds the tensile strength of the melts. Some evidence has suggested that this effect results in shark skin rather than melt fracture. The last theory is wall slip theory. The consensus opinion amongst rheologists is the melt fracture arises due to the slippage of the melt at the die wall. One of the reasons for this is evident in the behavior of high density polyethylene in which the experimental rheological observation with the HDPE melts reveal a discontinuity in the flow curve.

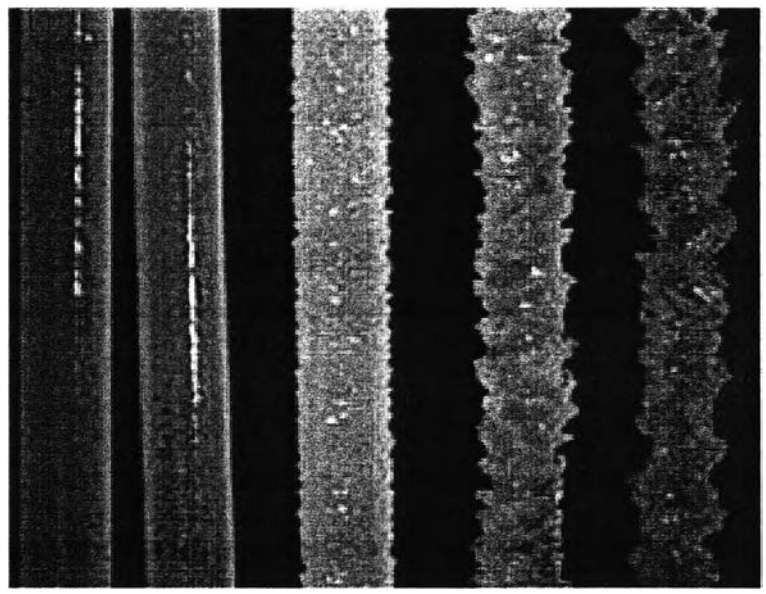

Figure 2.9 Example of melt fracture.

2.2 Literature Surveys

Shu-Ying Gu *et al.* (2004) investigated the rheology of polypropylene-clay nanocomposites on parallel plate rheometer. It was found that the storage moduli, loss moduli, and dynamic viscosities of polymer/clay nanocomposites increase monotonically with organophilic-mont-morillonite(org-MMT) content, and the presence of the organo-clay leads to a pseudo-solid-like behavior. The polymer/clay nanocomposites melts show the greater shear thinning tendency than pure PP melts because of the preferential orientation of the MMT layers. Therefore, polymer/clay nanocomposites have high moduli, with improved processibility in comparison with pure PP.

Chi-Ming Chan *et al.* (2002) prepared nanocomposites from polypropylene reinforced with calcium carbonate nanoparticles (average particle size = 44 nm). The dispersion of $CaCO_3$ was good when the filler content was below 9.2 %vol. DSC result indicated that $CaCO_3$ was an effective nucleating agent for iPP and the incorporate of the nanoparticles increased the tensile modulus by as much as 85%, while the ultimate stress and strain, as well as yield stress and strain, were not much affected by the presence of $CaCO_3$ nanoparticles.

Incarnato *et al.* (2004) studied the rheological behavior of polyamide-based nanocomposites produced by melt compounding using three different silicate loading on dynamic frequency sweep, steady rate sweep and stress relaxation tests in term of the effect of the kind of matrix and clay content. The results showed that, the rheology highly sensitive to the nanoscale structure of the materials, put out the pseudo-solid like flow behavior at long time in the hybrids with silicate content higher than 6 %wt and produced with high extrusion rate; this respond was related to the formation of an extended structural network across the polymer matrix due to strong polymer-silicate interactions that slow the relaxation times of the macromolecules.

Fornes *et al.* (2001) using the organoclay nanocomposites based on three different molecular weight grades of nylon 6 were prepared by melt processing using a twin screw extruder. The results suggested that the tensile modulus and yield strength were found to increase with increasing concentration of clay, while elongation at break decreased. Differences in properties between the three types of composites were attributed to differences in melt rheology. Capillary and dynamic parallel plate data revealed sizeable differences in the levels of shear stress between each nanocomposites system.

Liang, (2002) investigated the rheological properties of polymer-filled glass beads. The result showed that the die-swell behavior and distance pressure drop of polypropylene (PP) filled with glass beads were investigated by using of the sample melts. The die-swell was increased linearly with the increase of shear stress at the wall.

Lei *et al.* (2002) studied the time dependent behavior of LDPE filled with TiO_2 on the dynamic stress rheometer at a certain temperature, frequency, and stress the dynamic time sweep test was conducted. Experimental temperatures 180, 190, and 200^{o}C; experimental frequencies 0.5, 10 and 100 rad/s; and experimental stresses 20000, 40000, 80000, and 90000 dyn/cm^2 were employed. It was found the viscosity slightly decreased with time at first, then continuously decreased with time. The 30 wt% of TiO_2 content was critical to obvious time-dependence behavior. The viscosity increase with time was related to the formation of hard shell around the melt sample during the test.

White and Tanaka (1981) investigated the elongtional flow and melt spinning instability of the small particles as carbon black, TiO_2, and $CaCO_3$ filled with PS matrix. It is suggested that the existence of yield values in the elongational viscosity of concentrated suspensions of small particles in polymer melts leads to enhanced instability of uni-axial stretching and melt-spinning behavior. Segregated groups of particles could be a stress concentrator which would lead to premature failure.